Static dielectric constant of thin dielectrics in extremely scaled silicon nanosheet transistors

Massimo V. Fischetti [1,*] Dallin O. Nielsen [1] and Edward Chen [2]
[1] *Department of Materials Science and Engineering, The University of Texas at Dallas, 800 W. Campbell Road, Richardson, Texas 75080, USA*
[2] *Corporate Research, Taiwan Semiconductor Manufacturing Company Ltd., 168, Kehuan Rd., Hsinchu Science Park, Hsinchu 308-001, Taiwan*

(Received 31 July 2026; revised 30 September 2026; accepted 27 October 2026; published 6 November 2026)

We argue that the static dielectric constant of small (thin and/or narrow) semiconductor and insulator nanostructures depends strongly on their environment. We do so by considering the electronic response, simply reviewing, briefly but critically, the existing literature. Regarding the ionic response, in addition to reviewing the literature, we use a simple model to account for the confinement of optical phonons in thin films and show that the reduction of their density of states has a negligible effect on the dielectric constant, in contrast to some claims found in the literature. In general, we argue that in realistic structures, such as double-gated Si nanosheets, the use of the bulk dielectric constants for both the channel and the gate insulators is justified.

DOI: 10.1103/gx65-fjlr

I. INTRODUCTION

The continuing scaling of semiconductor devices requires the use of thinner semiconductor and insulating films. For example, the field effect transistors of the present 2–3 nm node employ channels consisting of Si nanosheets as thin as three unit cells (≈1.5 nm) [1] and (double) gate-insulator stacks consisting of a 0.6-nm-thick SiO_2 layer and a 1.2-nm-thick HfO_2 film [1–4]. In the study of the electrostatic and charge-transport properties of these devices, the question arises whether the dielectric properties of these films (specifically, their static dielectric constant) are affected by their reduced thickness. Obviously, quantum confinement changes the electronic band structure as electrons must be considered as a two-dimensional electron gas. However, also their dielectric properties change when considering very thin films. Since the dielectric response of a crystal is due to its electronic and ionic polarization, in thin films we may expect a different electronic response due to the change of the bandgap, usually increasing in thinner films, and a change of the ionic response due the different density of states of the optical phonons that may be geometrically confined.

Here, we intend to discuss these issues in general terms, considering the covalent Si and polar SiO_2 and HfO_2 as specific examples, dealing separately with these two types of polarization: the electronic polarizability (that controls entirely the dielectric response of covalent crystals, such as

*Contact author: max.fischetti@utdallas.edu

Published by the American Physical Society under the terms of the Creative Commons Attribution 4.0 International license. Further distribution of this work must maintain attribution to the author(s) and the published article's title, journal citation, and DOI.

indeed Si) and the ionic response that plays a large role in controlling the dielectric constant of polar insulators (defining as "polar" those noncovalent crystals that exhibit infrared-active phonons that contribute to the static dielectric constant). To anticipate and summarize the main conclusion from a survey of the literature, looking at both experimental and theoretical works, the static dielectric constant of thin films of semiconductors or insulators decreases with decreasing thickness when considering isolated, freestanding films. However, in films embedded in other solids, such as Si supported and/or gated by SiO_2 or HfO_2, the dielectric constant changes only by a small amount. Interface effects, such as surface polarization or the presence of interfacial layers, may even increase it for both semiconductors and insulators: In short, the polarizability of a free surface is reduced by the proximity of the vacuum, but it may even be boosted by the proximity of a medium with a higher polarizability. Overall, we do not think that it is a major effect.

II. ELECTRONIC RESPONSE

The electronic dielectric properties of thin Si films have been investigated both experimentally and theoretically. Experimentally, Yoo and Fauchet [7] using ellipsometry have observed a reduction from its bulk value of the dielectric constant of thin (100) Si films on SiO_2 from $\approx 11.9\epsilon_{vac}$ (where ϵ_{vac} is the permittivity of vacuum) in bulk Si to about $10.2\epsilon_{vac}$ in 2-nm-thick Si films. Theoretically, the study is quite complicated and indeed the literature shows inconsistent results: Using density functional theory (DFT) in the local density approximation, Shi and Ramprasad [8] have not predicted any depression of ϵ_{Si} even in (111) Si films as thin as 1 nm. Specifically, they have employed Si-SiO_2 and Si-HfO_2 supercells (1.096-nm-thick Si and 1.47-nm-thick SiO_2 in the β-cristobalite structure, and 1.99-nm-thick HfO_2 in the tetragonal structure), obtaining a static dielectric constant of about $12\epsilon_{vac}$ for Si, about $4\epsilon_{vac}$ for SiO_2 and $16\epsilon_{vac}$ for HfO_2 (whose bulk value in tetragonal is about the same). They also observed an increasing polarization of Si and oxides at the interfaces. Similar results have been obtained by Giustino *et al.* [9], who have calculated a moderate reduction, about $8\% \pm 1\%$, of ϵ_{Si} in 1.5 nm Si layers surrounded by SiO_2. Whereas these results have been obtained considering Si films surrounded by dielectrics, a depression of ϵ_{Si} has been predicted when considering freestanding Si sheets. For example, Kageshima and Fujiwara [10,11] have used DFT with the generalized gradient approximation (GGA) to study H-terminated freestanding (111) Si films obtaining a significant depression of the Si dielectric constant, as large as a factor of 4, for the out-of-plane dielectric constant; specifically, the in-plane value of ϵ_{Si} remains constant at around $13.5\epsilon_{vac}$, whereas its out-of-plane value drops from $12.5\epsilon_{vac}$ to $6.6\epsilon_{vac}$ as the Si thickness is reduced from ten bilayers to one bilayer. Similarly, Delerue and Allan [12] considered single layers of cubic and spherical Si nanocrystals using self-consistent tight binding and found that ϵ_{Si} is reduced from its bulk value and is strongly influenced by the morphology of the nanostructure. Judging from these results, one may speculate that indeed the dielectric environment and the morphology of the interfaces significantly affect the dielectric response and that a thin film may inherit to some extent the polarization properties of the surrounding environment. This is confirmed by the fact that Ref. [8] shows that thin Si films surrounded by SiO_2 and HfO_2 exhibit an ionic response, presumably induced by the surrounding oxides. Moreover, even Yoo and Fauchet [7] observe a significant effect of the polarization of the surface; in their samples, this is the Si-air interface and this may cause the moderate reduction of ϵ_{Si} that they observe. Similarly, our own work (unpublished work for Si but published for graphene and graphene nanoribbon [5]) based on the random phase approximation (RPA) within an empirical-pseudopotential approximation shows a very strong reduction of the static, long-wavelength dielectric tensor in ultrasmall freestanding (100) Si nanowires. This is shown in Fig. 1. The experimental results of Refs. [7,11],[12] are also shown in Fig. 2.

It may be tempting to view the increasing bandgap as the main (or only) cause of the reduction of the dielectric constant in thin films: Indeed, considering the static, long-wavelength limit of the well-known Lindhart expression for the polarization of the valence electrons in a dielectric [see

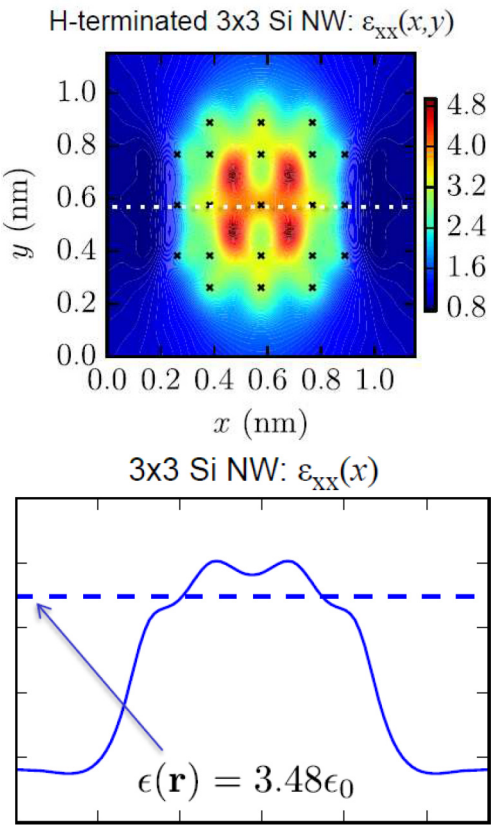


FIG. 1. Top: Contour plot of the local dielectric constant of a freestanding 3 × 3 cells Si nanowire calculated using the method described in Ref. [5]. Bottom: The same but along the cut shown by the dashed line at left. Note how the dielectric constant is reduced significantly from its bulk value. Presumably, this is due to the fact that the nanowire is surrounded by vacuum. The presence of a high-κ dielectric is likely to increase the polarizability of the nanowire, thus increasing its dielectric constant, as one may infer from the literature [6].

Eq. (11.42) of Ref. [13]], we have

$$\epsilon(\mathbf{q}=0;\omega=0) \approx \epsilon_{\text{vac}}\left[1+\left(\frac{\hbar\omega_{\text{v,P}}}{E_{\text{gap}}}\right)^2\right], \tag{1}$$

where $\omega_{\text{v,P}}$ is the frequency of the valence plasmons and E_{gap} is the bandgap. Therefore, we may expect that in thin films a larger bandgap may reduce the dielectric constant approximately by the ratio $E_{\text{gap}}^{(\text{bulk})}/E_{\text{gap}}^{(\text{film})}$. The main complications are due to the fact that the bandgap E_{gap} appearing in this equation is the average of the direct gap throughout the entire Brillouin zone, weighted by the joint valence-conduction density of states. In thin films, the bandgap may even decrease as the bulk Brillouin zone is projected onto the two-dimensional (2D) plane. This is the case of Si that acquires a small direct bandgap at the symmetry point $\overline{\Gamma}$. Therefore, only detailed and accurate band structure calculations of the RPA expression can provide an answer and the well-known problems that affect DFT calculations of the bandgap render the task quite hard. Moreover, in thin films, quantum confinement may affect the result. We may also expect that the wavelength dependence of 2D plasmons, intersubband plasma excitations, and surface polarization may play a significant role.

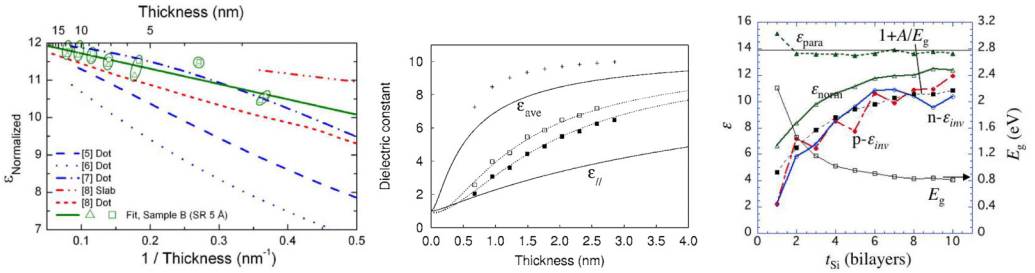


FIG. 2. Left: Static dielectric constant of thin freestanding Si films plotted as a function of film thickness. The experimental data, obtained from ellipsometry, are shown by the open green symbols and the thick green line. Results from various theoretical models for Si quantum dots and thin films are also shown. [Reprinted with permission from Ref. [7], ©2008 by the American Physical Society.] Center: "*Effective dielectric constant* ϵ_M *of Si quantum wells (+) and of layers of cubic Si nanocrystals separated by a vacuum gap of 2.7 Å (open squares) and 4.1* Å *(solid squares) calculated in tight binding. The dotted line is the fit of these data using Eq. (1). The continuous lines represent the average dielectric constant* ϵ_{ave} *and the dielectric constant* $\epsilon_{\parallel}$ *of capacitors in parallel.*" [Figure and words in quotes/italic reprinted with permission from Ref. [12], ©2006 by the American Physical Society.] Right: "*Channel thickness* t_{Si} *dependence of various dielectric constants.* p-ϵ_{inv} *and* n-ϵ_{inv} *are the inversion-layer dielectric constants* ϵ_{inv} *for the p- and the n-channel. All results are at* $V_G = \pm 3$ V. ϵ_{para} *and* ϵ_{norm} *are the static electric parts of the optical dielectric constants* ϵ_{opt} *for incident light with different polarization. Also shown, the channel thickness* t_{Si} *dependence of the band gap* E_g." [Figure and words in quotes/italic reprinted/adapted with permission from Ref. [11], ©2010 by the American Institute of Physics.]

In any event, the experimentally observed drop of the static dielectric constant is limited to less than 20% in Si sheets as thin as three cells. Therefore, assuming the bulk Si value for the dielectric constant of thin Si nanosheets is not going to significantly affect the results of any calculation, as it is a variation smaller than the uncertainties due to the many other approximations that must be embraced in most cases.

III. IONIC RESPONSE

In insulators, the electronic response shows the same reduction expected for semiconductors. However, given their larger bandgap, quantum electronic confinement has a much smaller effect. Indeed, Di *et al.* [14] have measured for the bandgap of HfO_2 values increasing only by about 3% as the thickness decreases from 4 to 2 nm. The issue is also complicated by the fact that HfO_2 can crystallize in various forms, monoclinic, tetragonal, orthorhombic, or cubic, each exhibiting a different bandgap. This complicates the issue of understanding the behavior of these amorphous hafnia films.

From these considerations, it is safe to assume that the possible dependence of the dielectric constant on the thickness of polar insulators is determined mainly by their ionic response. A review of the literature regarding the effect of thickness and phonon confinement on the dielectric constant, ϵ_{ox}, of thin insulators shows inconsistent experimental trends and theoretical predictions. Experimentally, some studies have shown the expected reduction of ϵ_{ox} in thin films. For example, Ref. [15] shows a drop of ϵ_{ox} from $21.3\epsilon_{vac}$ to $8\epsilon_{vac}$ in HfO_2 films as their thickness is reduced from 98.6 to 13.5 nm. Similarly, Zhang *et al.* [16] have reported a drop of the dielectric constant with a decreasing thickness of Ta_2O_5/HfO_2, Ta_2O_5/ZrO_2, and ZrO_2/HfO_2 nanolaminates. On the contrary, Perkins *et al.* [17] and Chang *et al.* [18] have hinted at the possible observation of a higher ϵ_{ox} in thin ZrO_2 and SiO_2 films. Theoretical calculations show the same inconsistency: For example, Giustino, Umari, and Pasquarello [9] have used DFT to study the Si-SiO_2 system, showing a slight increase of the SiO_2 dielectric constant (static and optical) in ultrathin films ($t_{ox} \lessapprox 0.7$ nm).

They attribute this result to the presence of a 0.32-nm-thick interfacial layer with a static dielectric constant of $7.1\epsilon_{\rm vac}$. This is due to the gradient of the chemical composition going from Si to SiO_2 via a suboxide SiO_x ($x < 2$) transition layer and may also be the result of the increased polarizability of the SiO_2 ions due to the proximity of a material, Si, with a higher polarizability, as we mentioned before. They show that a classical three-layer model (Si/interface-suboxide/SiO_2) fits the DFT calculation with a 2% accuracy.

On the other hand, Zaccone [19] has recently predicted a dramatic reduction of the ionic component of dielectric constant of thin films of polar materials. Whereas Giustino *et al.* [9] stress the importance of interface polarization effects, especially in the interfacial suboxide transition layer, Zaccone reaches his conclusion on the truncation of the Debye phonon density of states (DoS) at the lower bound $\omega_{\rm min} = c_{\rm s}\pi/t_{\rm ox}$, where $c_{\rm s}$ is the sound velocity and $t_{\rm ox}$ is the film thickness. In general, the Debye model describes correctly the DoS of acoustic phonons. These may affect the dielectric response only via indirect, higher-order effects, such as the elasto-optic effect [20] (due to changes of the charge density in the crystal due to the strain associated with acoustic phonons), or Brillouin scattering [21] that may change the high-frequency response. However, acoustic phonons play a negligible role at the low frequencies of interest here: The static dielectric constant is determined almost exclusively by the optical phonons. Therefore, approximating the phonons' DoS with the Debye model may be correct in the case of dielectrics that exhibit extremely soft optical modes, such as barium strontium titanate ($Ba_xSr_{1-x}TiO_3$, BST), on which Zaccone is interested. However, when considering the "harder" insulators of interest here, the use of the Debye model appears inappropriate. Equally inappropriate seems to be the idea of setting a lower bound of the phonon frequency at $\omega_{\rm min} = c_{\rm s}\pi/t_{\rm ox}$, since the dispersion of the optical phonons is almost flat and does not vanish at long wavelengths. Thus, the dependence on $t_{\rm ox}$ of the static dielectric constant can only be due to the onset of discretized branches of confined optical phonons and Zaccone's conclusions cannot be extended to the insulators that are widely used in the nanoelectronic technology, such as SiO_2, Si_3N_4, Al_2O_3, or $HfiO_2$.

The results of the various articles mentioned here are summarized in Fig. 3. This figure shows the contrasting experimental and theoretical results regarding the dielectric constant of thin SiO_2 and HfO_2 films and Zaccone's results for BST. Here, we intend to (hopefully) clarify the situation by giving a proverbial "back-of-the-envelope" estimation of the reduction of the dielectric constant that we may expect (or not) from the confinement of optical phonons in thin films of polar insulators. Necessarily, but regretfully, we will have to ignore interface polarization and anisotropic effects whose treatment requires much more than the back of an envelope.

Let us start by considering bulk dielectrics, assumed isotropic (so that all vector fields defined below, $\boldsymbol{\delta}$, $\mathbf{D}$, $\mathbf{P}$, and $\boldsymbol{\rho}_{\rm pol}$, are aligned along the same direction, in-plane or out-of-plane, of the field $\boldsymbol{\mathcal{E}}$, and we will consider only their magnitudes). Equation (10) gives the frequency dependence of the long-wavelength dielectric function of polar crystals. Following roughly Zaccone's treatment of the problem [19], this expression can be obtained by considering a simple linear diatomic chain (mimicking a polar crystal) and noticing that, in the long-wavelength limit, the distance δ between the anion and the cation oscillates in time according to the simple harmonic equation of motion:

$$\frac{{\rm d}^2\delta(t)}{{\rm d}t^2} - \gamma\frac{{\rm d}\delta(t)}{{\rm d}t} + \omega_{\rm TO}^2\delta(t) = 0, \tag{2}$$

where $\omega_{\rm TO} = (D/\mu)^{1/2}$ is the long-wavelength frequency of the transverse optical phonons, D is the "spring constant," and, in the dielectric continuum limit, μ is the reduced mass of ions 1 and 2, $\mu^{-1} = m_1^{-1} + m_2^{-1}$. We have also included a "friction" term $-\gamma[{\rm d}\delta(t)/{\rm d}t]$, where $\gamma = 1/\tau_{\text{3-ph}}$, that mimics the finite lifetime $\tau_{\text{3-ph}}$ of the optical phonons due to their anharmonic coupling to the acoustic phonons. In the presence of an oscillating electric field, $\mathcal{E}e^{i\omega t}$, the anion-cation distance takes the form $\delta(t) = \delta_0(\omega)e^{i\omega t}$, where

$$\delta_0(\omega) = -\frac{e^*\mathcal{E}}{\mu}\frac{1}{\omega_{\rm TO}^2 - \omega^2 - i\omega\gamma}, \tag{3}$$

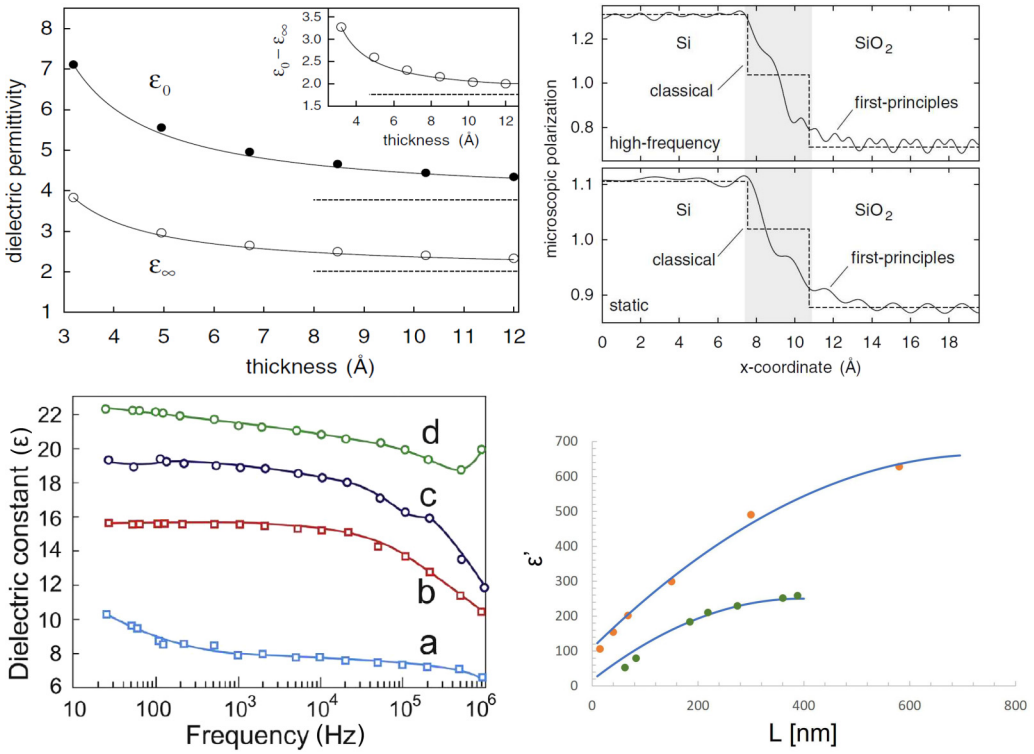


FIG. 3. Top left: Theoretically calculated permittivities "ϵ_∞ *(circles) and* ϵ_0 *(disks) of the oxide overlayer vs. its thickness, compared to the results of a classical three-layer model (solid). The classical two-layer model gives a constant permittivity corresponding to that of bulk* SiO_2 *(dashed). Inset: ionic contribution to* ϵ_0." Top right: "*High-frequency (upper panel) and static (lower panel) microscopic polarization along x (solid lines) compared to the classical three-layer model (dashed lines)*" [assuming the bulk values of ϵ_0 for Si and SiO_2]. "*The polarization is normalized by its average value in the cell. For the static polarization we used a Gaussian broadening of 0.9 Å to smear out the pointlike ionic contributions. The suboxide region is shaded.*" [Figures and words in quotes/italic reprinted with permission from Ref. [9], ©2003 by the American Physical Society.] Bottom left: Experimentally measured dielectric "*permittivity vs. frequency curves for different* HfO_2 *film*" (deposited on Si by sputtering and with unpassivated top surface) "*thicknesses: 13.5 nm (a), 29.6 nm (b), 48.8 nm (c), and 98.6 nm (d).*" [Figure and words in quotes/italic reprinted with permission from Ref. [15], ©2019 by the American Vacuum Society.] Bottom right: "*Comparison between the theoretical prediction given by Eq. (15), continuous line, and experimental data (circles). The latter are in arbitrary physical units, as customary for dielectric spectroscopy measurements. The upper curve refers to experimental data of dielectric permittivity of* $(Ba_{0.7}, Sr_{0.3})TiO_3$ *(BST) thin films measured at* $\omega = 4$ kHz *from Ref. [3], fitted by Eq. (15) with* $K_1 = 1.5$ *and* $K_2 = 0.001$, *and* $\epsilon_\infty = 100$. *The lower curve refers to experimental data of dielectric permittivity of* $(Ba_{0.5}, Sr_{0.5})TiO_3$ *thin films averaged between* $\omega = 400$ Hz *and* $\omega = 10$ kHz *from Ref. [25], fitted by Eq. (15) with* $K_1 = 1.2$ *and* $K_2 = 0.0015$, *and* $\epsilon_\infty = 10$. *All experimental measures were made at room temperature*." [Figure and words in quotes/italic reprinted with permission from Ref. [19] , ©2024 by the American Physical Society.]

with e^* being the effective charge of each dipole and ω_{TO} is the frequency of the transverse optical (TO) phonon. From now on, we will ignore the "broadening" γ, since it does not affect the main point of this discussion. For a volume density n_{dip} of anion-cation pairs, the polarization density (in

C/m^2) will be

$$\rho_{\rm pol}(\omega) = n_{\rm dip} e^* \delta_0(\omega) = -n_{\rm dip} \frac{e^{*2}\mathcal{E}}{\mu} \frac{1}{\omega_{\rm TO}^2 - \omega^2}. \tag{4}$$

Finally, the polarization field $P(\omega)$ will be (assuming a uniform $\epsilon^{(\infty)}$, the electronic component of the dielectric response)

$$P(\omega) = -\frac{\rho_{\rm pol}(\omega)}{\epsilon^{(\infty)}} = \frac{n_{\rm dip} e^{*2}\mathcal{E}}{\epsilon^{(\infty)}\mu} \frac{1}{\omega_{\rm TO}^2 - \omega^2}, \tag{5}$$

where $\epsilon^{(\infty)}$ is the dielectric constant at a frequency large enough for the phonons not to respond. This describes exclusively the electronic dielectric response. As a result, the displacement field D in this simple model will be

$$D(\omega) = \epsilon^{(\infty)}\mathcal{E} + \epsilon^{(\infty)} P(\omega) = \epsilon^{(\infty)}\mathcal{E}\left[1 + \frac{n_{\rm dip} e^{*2}}{\epsilon^{(\infty)}\mu} \frac{1}{\omega_{\rm TO}^2 - \omega^2}\right]. \tag{6}$$

In this equation, we can identify the dielectric function $\epsilon_{\rm ox}(\omega)$ as

$$\epsilon_{\rm ox}(\omega) = \epsilon^{(\infty)} + \frac{n_{\rm dip} e^{*2}}{\mu} \frac{1}{\omega_{\rm TO}^2 - \omega^2} = \epsilon^{(\infty)} + f \frac{\omega_{\rm TO}^2}{\omega_{\rm TO}^2 - \omega^2}. \tag{7}$$

The factor $f = n_{\rm dip} e^{*2}/(\mu\omega_{\rm TO}^2)$ is proportional to the oscillator strength of the phonons. It determines how the phonon response increases the dielectric response from $\epsilon^{(\infty)}$, at frequencies large enough so that the phonons do not respond, to a "static" value $\epsilon^{(0)}$ affected by the full ionic response. Therefore, we may recast Eq. (7) as

$$\epsilon_{\rm ox}(\omega) = \epsilon^{(\infty)} + (\epsilon^{(0)} - \epsilon^{(\infty)}) \frac{\omega_{\rm TO}^2}{\omega_{\rm TO}^2 - \omega^2}. \tag{8}$$

Considering the more realistic case of optical phonons with a dispersion $\omega'(\mathbf{q})$, then Eq. (7) becomes [cf. Eq. (8) of Ref. [19]]

$$\epsilon_{\rm ox}(\omega) = \epsilon^{(\infty)} + \int {\rm d}\omega'\, f(\omega')\mathcal{D}^{\rm (TO)}(\omega') \frac{\omega'^2}{\omega'^2 - \omega^2}, \tag{9}$$

where $\mathcal{D}^{\rm (TO)}(\omega)$ is the DoS of the TO phonons at frequency ω and $f(\omega)$ is their oscillator strength. This expression can be simplified by noticing that in most insulators the optical phonons exhibit a small dispersion. For example, because of the relatively small mass difference between Si and O, in SiO_2 $\mathcal{D}^{\rm (TO)}(\omega)$ exhibits two sharp phonon-DoS peaks at approximately 45–50 and 140–150 meV in both the α-quartz and β-cristobalite forms. Even though HfO_2 may exhibit a stronger dispersion, it is reasonable to ignore the TO dispersion altogether and consider an approximate TO DoS consisting of two Dirac deltas at two frequencies, $\omega_{\rm TO1} > \omega_{\rm TO2}$ [we shall convert the integral in Eq. (9) to a sum over discrete modes also in Eq. (11), when dealing with confined phonons]. Therefore, Eq. (9) can be approximated as

$$\epsilon_{\rm ox}(\omega) = \epsilon^{(\infty)} + (\epsilon^{\rm (mid)} - \epsilon^{(\infty)}) \frac{\omega_{\rm TO1}^2}{\omega_{\rm TO1}^2 - \omega^2} + (\epsilon^{(0)} - \epsilon^{\rm (mid)}) \frac{\omega_{\rm TO2}^2}{\omega_{\rm TO2}^2 - \omega^2}, \tag{10}$$

where $\epsilon^{\rm (mid)} - \epsilon^{(\infty)} = f_1$ and $\epsilon^{(0)} - \epsilon^{\rm (mid)} = f_2$ are the oscillator strengths of the two TOs.

What we wish to consider now is how Eq. (10) changes in thin insulating films. In principle, we expect that in these films the phonon DoS, $\mathcal{D}^{\rm (TO)}(\omega)$, will change, since the TO phonons are geometrically confined. Indeed, in a bulk insulator, the total oscillator strength arises from the contribution of all the TO bulk modes. So, for example, if we are interested in looking at the long-wavelength ionic response on the (x, y) plane of the crystal, TO phonons with any out-of-plane wave vector q_z will contribute to f. The dielectric function $\epsilon_{\rm ox}$ will be obtained from Eq. (10)

with a spatially constant dipole density $n_{\rm dip}e^*\delta_0$, as discussed above. However, in a thin film of thickness $t_{\rm ox}$ lying on the (x, y) plane, there will be only a discrete number of modes confined along the out-of-plane z direction that can contribute to the polarizability. The problem now consists in determining the fractional oscillator strength of each one of these modes.

Let us proceed as follows: Let us assume that the ionic displacement δ is clamped to zero at the surfaces/interfaces at $z = 0$ and $z = t_{\rm ox}$. This is the extreme worst-case scenario, since it will result in the lowest phonon density of states and so in the lowest dielectric constant. In this case, for each confined TO phonon we will have a spatially varying anion-cation separation $\delta(z)$ proportional to $\sin(q_{z,n}z)$, where $q_{z,n} = (2n + 1)\pi/t_{\rm ox}$ is the discretized wave vector of the TO phonon. Since we are interested in estimating the dielectric constant of the film averaged over its thickness, only symmetric modes (i.e., symmetric around the center of the film, corresponding to odd indices $2n + 1$) will give a nonvanishing contribution to the thickness-averaged polarization; therefore, we can ignore the antisymmetric/odd modes. Then, keeping in mind that, for a spatially varying polarization density $\boldsymbol{\rho}_{\rm pol}$, the polarization field $\mathbf{P}$ is given by $\nabla\cdot\mathbf{P} = -\rho_{\rm b}/\epsilon^{(\infty)} = -\nabla\cdot\boldsymbol{\rho}_{\rm pol}/\epsilon^{(\infty)}$ (where $\rho_{\rm b} = \nabla\cdot\boldsymbol{\rho}_{\rm pol}$ is the bound charge density), the ionic polarizability will result in a position-dependent long-wavelength local dielectric function $\epsilon_{\rm ox}(\omega, z)$:

$$\epsilon_{\rm ox}(\omega, z) = \epsilon^{(\infty)} + S_N(z)\left[(\epsilon^{(\rm mid)} - \epsilon^{(\infty)})\frac{\omega_{\rm TO1}^2}{\omega_{\rm TO1}^2 - \omega^2} + (\epsilon^{(0)} - \epsilon^{(\rm mid)})\frac{\omega_{\rm TO2}^2}{\omega_{\rm TO2}^2 - \omega^2}\right], \tag{11}$$

where the function $S_{N_{\rm s}}(z)$ that modulates the phonon oscillator strength is

$$S_{N_{\rm s}}(z) = \begin{cases} \frac{4}{\pi}\sum_{n=0}^{N_{\rm s}}\frac{1}{2n+1}\sin\left[\frac{(2n+1)\pi}{t_{\rm ox}}z\right], & \text{for } 0 \leqslant z < t_{\rm ox}, \\ 0, & \text{otherwise}, \end{cases} \tag{12}$$

where the fractional oscillator strength (or "weight") of each confined phonon is $4/[\pi(2n + 1)]$. This can be seen in two different (but mathematically equivalent) ways: As explained in detail in Ref. [22], this weight is the areal density of in-plane TO-phonon states for a given $q_{z,2n+1}$, normalized to the total density of modes. Alternatively, note that Eq. (12) is the simple Fourier-series expansion of a square wave. Therefore, Eq. (12) yields a constant value (unity) for $0 \leqslant z < t_{\rm ox}$. This gives the expected z-independent ionic polarization when summing over the infinitely many modes present in an infinitely thick film. In summary, Eq. (12) reflects the z-dependent dipole density, $n_{\rm dip}e^*\delta_0 S_{N_{\rm s}}(z)$, of confined TO phonons and yields the expected position-independent dielectric constant in an infinitely thick film (i.e., in the limit of a bulk dielectric as $N_{\rm s} \to \infty$) [23].

Obviously, the number of symmetric (even) modes, $N_{\rm s}$, appearing in the sum in Eq. (12) is determined by the number of even TO-phonon modes present in the structure. This is $N/2 - 1$, where N is the total number of TO phonons. For an layer $N_{\rm c}$-cell-thick layer with $N_{\rm a}$ atoms in each cell, we have $N = N_{\rm c}(N_{\rm a} - 1)$ out-of-plane and $N_{\rm c}(N_{\rm a} - 1)$ in-plane TO phonons. The oxides we are interested in are likely to be amorphous. However, considering them to be in some crystalline structure to get an estimate of the modes we should consider, $N_{\rm a} = 9$ for SiO_2 in the α-quartz structure and $N_{\rm a} = 24$ in the β-cristobalite structure. For HfO_2, $N_{\rm a} = 12$ in the orthorhombic, cubic, and monoclinic crystal structures, whereas $N_{\rm a} = 6$ in the tetragonal form. Therefore, in the limit of an infinitely thick film ($N_{\rm c} \to \infty$), $S_{N_{\rm s}}(z) \to S_\infty(z) = \theta(z) - \theta(z - t_{\rm ox})$, the "square-wave" function that is equal to 1 for $0 \leqslant z < t_{\rm ox}$, and zero otherwise. In this limit, $\epsilon_{\rm ox}(\omega, z)$ is the "usual" dielectric function, spatially constant in the film. However, considering thin SiO_2 films in the α-quartz structure (just to fix the ideas for an interesting case), the number of modes will be relatively small: $N_{\rm s} = 3$ (4 even modes) for a one-cell ($\approx$0.541 nm)-thick film; $N_{\rm s} = 7$ (8 even modes) for a two-cell ($\approx$1.08 nm)-thick film; and $N_{\rm s} = 11$ (12 even modes) for a three-cell ($\approx$1.62 nm)-thick film.

Figure 4 shows the z-dependent ionic component of the local dielectric "constant" $\epsilon_{\rm ion}(\omega = 0, z) = [\epsilon^{(0)} - \epsilon^{(\infty)}]S_{N_{\rm s}}(z)/\epsilon_{\rm vac}$ for SiO_2 films of thickness decreasing from four α-quartz cells ($\approx$2.16 nm) to one cell ($\approx$0.54 nm), assuming $[\epsilon^{(0)} - \epsilon^{(\infty)}]\epsilon_{\rm vac} = 1.4$, the bulk value. Although the dielectric constant vanishes at the surfaces of the films, an obvious consequence of the clamped

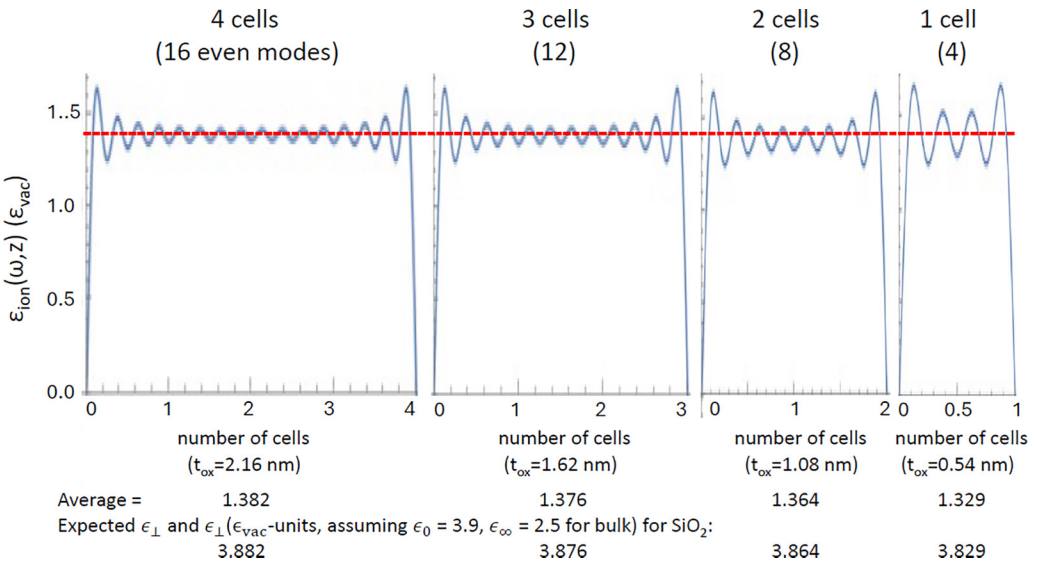


FIG. 4. Spatial dependence of the ionic component of the SiO_2 dielectric constant expressed by Eqs. (11) and (12) with the sum extended over the number of even TO modes in a (100) SiO_2 film with a thickness of four, three, two, and one cells (from left to right). Although fewer modes contribute in thinner films, the average dielectric constant, as shown assuming a thickness-independent electronic response, $\epsilon^{(\infty)}$), decreases only very slightly. The peaks seen at the surfaces of the layer are artifacts due to the Gibbs phenomenon. They may distort the results to some extent.

boundary conditions for the TO phonons, its average value remains very close to the bulk value: The polarizability is almost completely determined by the mode with the longest wavelength along the z direction (i.e., the $2n+1$ mode with $n=0$). This is because $8/\pi^2 \approx 81\%$ of the bulk ionic polarizability is due to this mode, thanks to the large number of in-plane states with such a small out-of-plane wave vector; as films become thinner and high-$(2n+1)$ modes are "lost," the effect of the phonon confinement is minor. As mentioned above, this is the worst-case scenario: If the TOs are freestanding or confined over a thicker region, the dielectric constant would be even closer to the bulk value. Moreover, the peaks observed near the surfaces in Fig. 4 are likely to be an artifact due to the Gibbs phenomenon. The net result of this "back-of-the-envelope" analysis is that the confinement of the TO phonons in thin insulators should not affect the dielectric constant in any significant way.

IV. CONCLUSIONS

We have argued that the static dielectric constant of thin semiconductor and insulator nanostructures is affected by the materials in which they are embedded. As fas as the electronic responses are concerned, we have reached this conclusion simply by reviewing published experimental and theoretical results. On the contrary, regarding the ionic response, we have used a simple "worst-case scenario" model to consider the reduced density of states of optical phonons in thin films to show that this has a negligible effect on their static dielectric constant. As a practical consequence of our study, we have argued that when studying the electrostatic and charge-transport properties of electronic devices scaled to sub-10 nm length, the use of the bulk dielectric constant is a satisfactory approximation.

ACKNOWLEDGMENTS

This work was supported by the Taiwan Semiconductor Manufacturing Company Ltd. (TSMC) TSMC#202001220021. We also thank the Texas Advanced Computing Center (TACC) for providing the computing resources required to perform this study and Texas Instruments for the Endowment that has provided additional financial support.

DATA AVAILABILITY

There are no publicly available research data or software supporting this manuscript. Requests for further information or data should be sent to the authors.

[1] A. Agrawal, W. Chakraborty, W. Li, H. Ryu, B. Markman, S. H. Hoon, R. K. Paul, C. Y. Huang, S. M. Choi, K. Rho, *et al.*, Silicon RibbonFET CMOS at 6 nm gate length, in *2024 International Electron Devices Meeting (IEDM), Technical Digest* (IEEE, San Francisco, California, 2024), Vol. 2024, pp. 1–4.

[2] N. Loubet, T. Hook, P. Montanini, C.-W. Yeung, S. Kanakasabapathy, M. Guillom, T. Yamashita, J. Zhang, M. X. J. Wang, *et al.*, Stacked nanosheet gate-all-around transistor to enable scaling beyond FinFET, in *Proceedings of the 2017 Symposium on VLSI Technology* (IEEE, Kyoto, Japan, 2017), pp. T230–T231.

[3] J. Park, W. Kim, S. Park, J. Yun, K. Hwang, J. Yang, D. Kim, J. W. Jeong, C. Yun, J. Bae, *et al.*, First demonstration of 3-dimensional stacked FET with top/bottom source-drain isolation and stacked n/p metal gate, in *2022 International Electron Devices Meeting (IEDM), Technical Digest* (IEEE, San Francisco, California, 2022), pp. 1–4.

[4] G. Yeap, S. S. Lin, H. L. Shang, H. C. Lin, Y. C. Peng, M. Wang, P. W. Wang, C. P. Lin, K. F. Yu, W. Y. Lee, *et al.*, 2 nm platform technology featuring energy-efficient nanosheet transistors and interconnects co-optimized with 3DIC for AI, HPC and mobile SoC applications, in *2024 International Electron Devices Meeting (IEDM), Technical Digest* (IEEE, San Francisco, California, 2024), Vol. 2024, pp. 1–4.

[5] J. Fang, W. G. Vandenberghe, and M. V. Fischetti, Microscopic dielectric permittivities of graphene nanoribbons and graphene, Phys. Rev. B **94**, 045318 (2016).

[6] J. Fang (unpublished).

[7] H. G. Yoo and P. M. Fauchet, Dielectric constant reduction in silicon nanostructures, Phys. Rev. B **77**, 115355 (2008).

[8] N. Shi and R. Ramprasad, Local properties at interfaces in nanodielectrics: An *ab initio* computational study, IEEE Trans. Dielectr. Electr. Insul. **15**, 170 (2007).

[9] F. Giustino, P. Umari, and A. Pasquarello, Dielectric discontinuity at interfaces in the atomic-scale limit: Permittivity of ultrathin oxide films on silicon, Phys. Rev. Lett. **91**, 267601 (2003).

[10] H. Kageshima and A. Fujiwara, First-principles study on inversion layer properties of double-gate atomically thin silicon channels, Appl. Phys. Lett. **93**, 043516 (2008).

[11] H. Kageshima and A. Fujiwara, Dielectric constants of atomically thin silicon channels with double gate, Appl. Phys. Lett. **96**, 193102 (2010).

[12] C. Delerue and G. Allan, Effective dielectric constant of nanostructured Si layers, Appl. Phys. Lett. **88**, 173117 (2006).

[13] M. V. Fischetti and W. G. Vandenberghe, *Advanced Physics of Electron Transport in Semiconductors and Nanostructures* (Springer Nature, Switzerland, 2016).

[14] M. Di, E. Bersch, A. C. Diebold, S. Consiglio, R. D. Clark, G. J. Leusink, and T. Kaack, Comparison of methods to determine bandgaps of ultrathin HfO_2 films using spectroscopic ellipsometry, J. Vac. Sci. Technol. A **29**, 041001 (2011).

[15] D. A. Golosov, N. Vilya, S. M. Zavadski, S. N. Melnikov, A. V. Avramchuk, M. Grekhov, N. I. Kargin, and I. V. Komissarov, Influence of film thickness on the dielectric characteristics of hafnium oxide layers, Thin Solid Films **690**, 137517 (2019).

[16] H. Zhang, R. Solanki, B. Roberds, G. Bai, and I. Banerjee, High permittivity thin film nanolaminates, J. Appl. Phys. **87**, 1921 (2000).

[17] C. M. Perkins, B. B. Triplett, P. C. McIntyre, K. C. Saraswat, S. Haukka, and M. Tuominen, Electrical and materials properties of ZrO_2 gate dielectrics grown by atomic layer chemical vapor deposition, Appl. Phys. Lett. **78**, 2357 (2001).

[18] H. S. Chang, H. D. Yang, H. Hwang, H. M. Cho, H. J. Lee, and D. W. Moon, Measurement of the physical and electrical thickness of ultrathin gate oxides, J. Vac. Sci. Technol. B **20**, 1836 (2002).

[19] A. Zaccone, Explaining the thickness-dependent dielectric permittivity of thin films, Phys. Rev. B **109**, 115435 (2024).

[20] S. H. Wemple and M. DiDomenico, Jr., Theory of the elasto-optic effect in nonmetallic crystals, Phys. Rev. B **1**, 193 (1970).

[21] B. I. Bennett, A. A. Maradudin, and L. R. Swanson, A theory of the Brillouin scattering of light by acoustic phonons in a metal, Ann. Phys. **71**, 357 (1972).

[22] To estimate the fractional oscillator strength of each confined mode, we may approximate the Brillouin zone of volume $\Omega_{\rm BZ}$ with a sphere of radius $q_{\rm BZ}$. Then, the density $\mathcal{D}^{\rm (TO)}_{\rm 2D}(2n+1)$ of TO-phonon states (per unit area) with out-of-plane (along the z direction) component of the wave vector equal to $q_{z,2n+1} = (2n+1)\pi/t_{\rm ox}$ is

$$\begin{aligned}\mathcal{D}^{\rm (TO)}_{\rm 2D}(2n+1) &= \frac{1}{(2\pi)^3}\int_{\Omega_{\rm BZ}} {\rm d}\mathbf{q}\,\delta(q\cos\theta - q_{z,2n+1}) \\ &= \frac{1}{(2\pi)^3} 2\pi \int_0^{q_{\rm BZ}} {\rm d}q q^2 \int_0^{\pi} {\rm d}\theta \sin\theta \delta(q\cos\theta - q_{z,2n+1}) \\ &= \frac{1}{(2\pi)^3} 2\pi \int_0^{q_{\rm BZ}} {\rm d}q q^2 \int_{-1}^{1} {\rm d}\mu \delta(q\mu - q_{z,2n+1}) \\ &= \frac{1}{(2\pi)^3} 2\pi \int_0^{q_{\rm BZ}} {\rm d}q q^2 \frac{1}{q_{z,2n+1}} = \frac{\Omega_{\rm BZ}}{2}\frac{t_{\rm ox}}{\pi(2n+1)}. \end{aligned} \tag{22.1}$$

Each mode contributes to the dielectric function with a z dependence of the form $\sin[(2n+1)\pi z/t_{\rm ox}]$ that, averaged over the thickness of the film, yields $2/[(2n+1)\pi]$. Therefore, the total density of TO modes that contribute to the dielectric function of an infinitely thick film will be

$$\begin{aligned}\mathcal{D}^{\rm (TO)}_{\rm tot,\infty} &= \sum_{n=0}^{\infty} N_{\rm 2D}(2n+1) = \frac{\Omega_{\rm BZ}}{2}\sum_{n=0}^{\infty}\frac{t_{\rm ox}}{(2n+1)\pi}\frac{2}{(2n+1)\pi} = \frac{\Omega_{\rm BZ}}{2}t_{\rm ox}\frac{2}{\pi^2}\sum_{n=0}^{\infty}\frac{1}{(2n+1)^2} \\ &= \frac{\Omega_{\rm BZ}}{2}t_{\rm ox}\frac{2}{\pi^2}\frac{\pi^2}{8} = \frac{\Omega_{\rm BZ}}{2}t_{\rm ox}\frac{1}{4}. \end{aligned} \tag{22.2}$$

Normalizing this contribution to unity for an infinitely thick film, each out-of-plane mode $2n+1$ (with a discretized out-of-plane wave vector $(2n+1)\pi/t_{\rm ox}$) carries the fractional oscillator strength (its "weight"):

$$\frac{\mathcal{D}^{\rm (TO)}_{\rm 2D}(2n+1)}{\mathcal{D}^{\rm (TO)}_{\rm tot,\infty}} = \frac{4}{\pi}\frac{1}{2n+1}, \tag{22.3}$$

which appears in Eq. (12). These "weights" are just the coefficients of the Fourier series of a square wave with unit amplitude. Equation (22.2) shows that the $2n+1$ mode gives an $(8/\pi^2)/(2n+1)^2$ contribution to $\mathcal{D}^{\rm (TO)}_{\rm tot,\infty}$ and so to the total polarization. Therefore, the first confined mode ($n=0$) gives an $8/\pi^2 \approx 81.1\%$ contribution, the second mode ($n=2$, $2n+1=3$) gives an $(8/\pi^2)/9 \approx 9\%$ contribution, the third mode gives$(8/\pi^2)/25 \approx 3.2\%$, the fourth mode gives $(8/\pi^2)/49 \approx 1.9\%$, and so on. Therefore, the dielectric constant is determined to a very large extent by the "ground-state" confined TO phonon so that it exhibits a very weak dependence on the thickness of the film.

[23] Strictly (and perhaps pedantically) speaking, this limit of "infinite thickness" relies on treating phonons as undamped, coherent plane waves, as stated after Eq. (3), as assumed in Eq. (12), and as also assumed by the Debye or Einstein models. We consider anharmonic effects that broaden and smear

the phonon density of states (by causing a finite phonon lifetime) as perturbations that do not alter our conclusions: Indeed, in Ref. [24] we estimate the coherence length of optical phonons to be on the order of 10 nm or more for Si, but values of the same order of magnitude or larger (from a few nanometers to tens of nanometers) are found for most solids, including semiconductors [25] and insulators (see, for example, Ref. [26] for α-quartz), thus covering the range of small thickness of interest in this discussion.

[24] M. V. Fischetti, D. O. Nielsen, and E. Chen, On the electronic and vibrational dimensionality of nanometer-scale silicon structures, arXiv:2608.18277.

[25] J. P. Freedman, J. H. Leach, E. A. Preble, Z. Sitar, R. F. Davis, and J. A. Malen, Universal phonon mean free path spectra in crystalline semiconductors at high temperature, Sci. Rep. **3**, 2963 (2013).

[26] P. Kharel, G. I. Harris, E. A. Kittlaus, W. H. Renninger, N. T. Otterstrom, J. G. E. Harris, and P. T. Rakich, High-frequency cavity optomechanics using bulk acoustic phonons, Sci. Adv. **5**, eaav0582 (2019).